Sverdlovsk revisited: Modeling human inhalation anthrax

Dean A. Wilkening*

Center for International Security and Cooperation, Stanford University, Stanford, CA 94305-6165

Edited by John M. Coffin, Tufts University School of Medicine, Boston, MA, and approved March 27, 2006 (received for review November 3, 2005)

Several models have been proposed for the dose–response function and the incubation period distribution for human inhalation anthrax. These models give very different predictions for the severity of a hypothetical bioterror attack, when an attack might be detected from clinical cases, the efficacy of medical intervention and the requirements for decontamination. Using data from the 1979 accidental atmospheric release of anthrax in Sverdlovsk, Russia, and limited nonhuman primate data, this paper eliminates two of the contending models and derives parameters for the other two, thereby narrowing the range of models that accurately predict the effects of human inhalation anthrax. Dose–response functions that exhibit a threshold for infectivity are contraindicated by the Sverdlovsk data. Dose-dependent incubation period distributions explain the 10-day median incubation period observed at Sverdlovsk and the 1- to 5-day incubation period observed in nonhuman primate experiments.

bioterrorism | dose–response function | incubation period

Concern that a terrorist group might attack civilian populations by releasing deadly pathogens, in particular anthrax, into the air has grown in the past decade. *Bacillus anthracis*, a Gram-positive, spore-forming bacillus ≈1 μm × 5 μm in size has long been a preferred agent for state biological weapons programs. *B. anthracis* can exist in the soil for decades and commonly infects herbivores, especially domesticated cattle, horses, and sheep. Three exposure pathways can infect humans: contact with contaminated animal products (cutaneous anthrax), ingesting contaminated meat (gastrointestinal anthrax), and inhalation of anthrax spores. If inhaled, *B. anthracis* can be quite lethal, on the order of 80–90% for the most virulent strains. Airborne delivery has been the focus of most biological weapon programs because of the possibility for mass casualties (1).

Anthrax is one of the most extensively researched biological warfare agents (2–6). Nevertheless, important aspects of the disease remain poorly understood, in particular, the human response to low-dose exposure and the temporal progression of the disease, especially the dose dependence of the incubation period. These issues have a significant influence on at least four bioterrorism policy issues.

First, the number of people infected by an atmospheric release depends on the dose–response function, particularly at low doses, because these exposures account for most of the infected victims unless a threshold exists below which infection does not occur. Predicting the consequences of a bioterrorist attack is important for sizing the Strategic National Stockpile (formerly the National Pharmaceutical Stockpile) and for estimating the level of medical logistics required to respond to a given anthrax release scenario.

Second, the time at which the first victims become symptomatic depends on the early time tail of the incubation period distribution. This tail determines the time at which astute physicians, or possibly syndromic surveillance systems, might detect the beginning of an anthrax outbreak in the absence of data from environmental sampling.

Third, the efficacy of appropriate medical intervention depends largely on its speed relative to the rate at which victims become symptomatic and, subsequently, pass into the prodromal and fulminant phases of the disease. Medical prophylaxis can be effective if administered before the appearance of symptoms, and it can be partially effective during the prodromal phase if accompanied by adequate supportive care. The incubation period distribution depends on host population susceptibility (e.g., age, gender, and health status) and the dose to which victims are exposed (Figs. 8 and 9, which are published as supporting information on the PNAS web site). Thus, modeling the dose-dependence of the incubation period and the duration of the prodromal period is crucial for assessing the effectiveness of different medical intervention strategies.

Finally, the residual risk posed by anthrax surface contamination depends on the dose–response curve at low doses. The greater the probability of infection at low doses, the greater the need for effective decontamination.

Four Inhalation Anthrax Models

Several models have been proposed to describe the dose–response function for human inhalation anthrax. Only two of these models are consistent with existing data. The accidental release of anthrax from a military compound in Chkalovsky, the southern most district of Sverdlovsk (now Yekaterinberg), Russia, in 1979, which led to the death of at least 70 people, is the best existing source of data on low-dose human exposure to inhalation anthrax from which to assess the accuracy of these models (7–9).

The lethal dose at which 50% of an untreated exposed population would die (LD_{50}) from inhalation anthrax is believed to be between 2,000 and 55,000 spores, with a nominal value of 8,000–10,000 spores (10). To explore the functional form of these different models, all are assumed to have the same LD_{50}, or ID_{50}, the dose at which 50% of the exposed population becomes infected, because nearly all untreated victims die.

Model A assumes the probability of infection follows a cumulative log-normal distribution with an ID_{50} of 8,600 spores and a PROBIT slope of 0.67 (11). Model B is similar, but with a probit slope of 1.43 (12, 13). Model C also assumes a cumulative log-normal distribution, but with a PROBIT slope of ≈2.4 and an age-dependent ID_{50} (14). The rationale for an age-dependent dose–response function is discussed in the *Supporting Text*, which is published as supporting information on the PNAS web site. This model yields ID_{50} values between 8,000 and 10,000 spores, depending on the demography one assumes.

Several researchers have proposed exponential dose–response functions for inhalation anthrax, which result if one assumes that spores act independently in infecting a host (15–17). Model D represents an exponential distribution derived by assuming a competing-risks model that takes into account the probability of spore destruction and spore germination in the lungs (17). This model also predicts the incubation period distribution, discussed below. In Model D, a spore clearance rate due to a combination of cilia action and macrophage destruction, θ, equal to 0.109 per day and a spore germination rate, λ, equal to 8.8×10^{-6} per day

Conflict of interest statement: No conflicts declared.

This paper was submitted directly (Track II) to the PNAS office.

*E-mail: wilkening@stanford.edu.

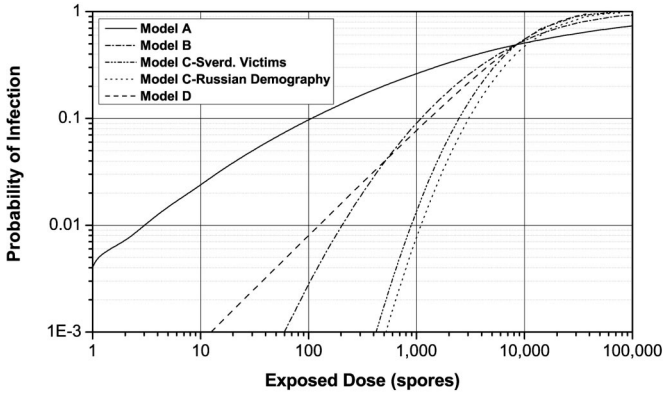

Fig. 1. Four inhalation anthrax dose–response functions ($ID_{50} \cong 8{,}600$ spores).

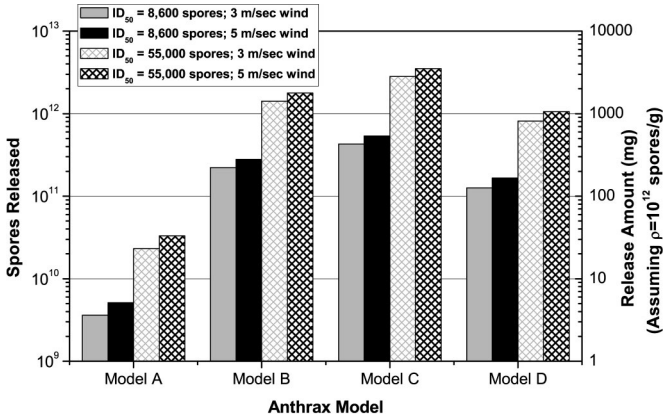

Fig. 2. Anthrax released to reproduce the Sverdlovsk outbreak.

yield an ID_{50} of ≈8,600 spores. Webb and Blaser (18) develop an age-dependent logit model for the dose–response function; however, this model is nearly identical to model D at low doses, with the appropriate choice of parameters and, hence, is not explored further here.

Fig. 1 illustrates these four dose–response models by using a logarithmic scale to highlight the different low-dose predictions. Model C is calculated for two demographic distributions: the age distribution of the Sverdlovsk victims and Russian demography circa 1979. Model A predicts greater infectivity at low doses relative to Model D because lognormal models reflect the susceptibility of a heterogeneous population, whereas exponential models assume independent spore action and homogeneous population susceptibility.

Reproducing the Spatial Distribution of Victims at Sverdlovsk

To determine which model is most accurate, especially at low doses, one can calculate which model most accurately reproduces the spatial distribution of cases observed in the Sverdlovsk outbreak. The spatial distribution is determined by simulating the atmospheric release of an amount of each type of anthrax to produce 81 infected victims, the estimated number of infected cases if the total fatalities were 70, thus normalizing the release amount for each model to reproduce the Sverdlovsk outbreak.[†] The population density for Sverdlovsk was obtained from the LandScan 2000 database, which provides world population on a 30 arc-second grid (≈1 km^2 at the equator; www.ornl.gov/sci/landscan/index.html).

Fig. 2 illustrates, for each model, the number of viable anthrax spores that must be released in a respirable size range (1–5 μm) to infect 81 individuals.[‡] The mass of material released in the 1- to 5-μm size range is also shown, assuming a dry anthrax preparation with 10^{12} spores per g (a very high density appropriate for an advanced biological weapon program, if produced in quantity).[§] These calculations agree, within the uncertainties associated with different input parameters, with Meselson's calculations for similar dose–response models (7, 21). Lower densities require proportionally larger release amounts; e.g., if the spore density is assumed to be 5×10^{10} spores per g and only 30% the material contained anthrax spores in the 1- to 5-μm size range, then the release amount for model A anthrax would be between 0.25 and 2.3 grams to reproduce the Sverdlovsk outbreak, depending on the wind speed and ID_{50} value assumed.

Sensitivity analysis was performed by using two ID_{50} values (8,600 spores and 55,000 spores) and surface wind speeds of 3.0 m/sec (the World Meteorological Organization Station 284400 value) and 4.9 m/sec (the Koltsovo Airport measurement). Wind speed does not have much effect on the number of spores that must be released to infect 81 people, but the ID_{50} value does. Other parameters could be varied; however, normalizing the release amount to produce 81 victims eliminates most of the variations one would expect.

Fig. 3 illustrates the predicted cumulative distribution of victims as a function of downwind distance when the amount of anthrax released of each type is that required to produce 81 infected victims, with an ID_{50} of 8,600 spores and a surface wind speed of 4.9 m/sec. The Sverdlovsk data, taken from Meselson *et al.* (7), is shown for comparison. Fig. 10, which is published as supporting information on the PNAS web site, illustrates pictorially the spatial extent of each plume. Only models A and D come close to predicting the correct spatial distribution of Sverdlovsk victims, with model A performing somewhat better. An uncertainty in the exact source location within compound 19 could account for as much as 0.25 km of the discrepancy shown in Fig. 3.

Models A and D are more accurate because their dose–response curves are less steep. Steep dose–response curves cannot produce extended spatial distributions, as one can see by considering the limiting case of a step-function dose–response curve with an ID_{50} of 8,600 spores. In this case, all isopleths collapse into one. Everyone inside this curve becomes infected, whereas no one outside is infected. Using such a dose–response curve to reproduce

[†]The Sverdlovsk anthrax is assumed to be 86 percent lethal for untreated victims.

[‡]These calculations used the Hazard Prediction and Assessment Code (Version 3.2) and archived World Meteorological Organization data for the Sverdlovsk region between April 2 and April 3, 1979. Limited vertical temperature profile data came from World Meteorological Organization Station 284400 located near Chkalovsky (listed alternately at 56.80N, 60.63E or 56.73N, 61.07E), and surface meteorology came from Koltsovo airport ≈15 km to the west-southwest of the release site. The release time is assumed to be approximately 1400 hours local time, on Monday, April 2 (7, 8, 20). The weather on April 2 was clear, with surface temperatures ≈-5°C and a fairly strong temperature inversion at an altitude of ≈1,200 m. The release location is assumed to be 7 m above the surface of the earth at 56.7825N, 60.5829E, a point inside the military compound from which the plume is believed to have originated. The breathing rate is assumed to be 30 liters/min, a rate appropriate for light work. The daytime environmental decay rate for anthrax spore viability (≈0.01 h^{-1}), and the deposition velocity for spores 5 microns in diameter (≈7 m/h) have little impact on the spore concentration 5 km downwind from the release point.

[§]General Yevstigneyev, Scientific Director of Compound 19 in the 1980s, stated that experiments to test vaccine efficacy were conducted on nonhuman primates at Compound 19 and that these tests used ≈5 billion spores and no more than 40 billion spores (8). Interestingly, this number corresponds to the amount of anthrax required to reproduce the Sverdlovsk outbreak by using model A. General Yevstigneyev, however, disagreed that the outbreak originated from Compound 19 because, according to him, experiments were not conducted in early April 1979, and the anthrax-laden air passed through two disinfecting stages and two filtration stages before being vented outside. Without more detailed evidence, one can only speculate that the venting from one test chamber through faulty filtration and disinfecting stages might have caused the anthrax outbreak. Alibek (20) maintains that the accident occurred because of a missing filter in an anthrax drying facility that was part of an anthrax production line, with no mention of vaccine efficacy tests and multiple filters and disinfecting stages.

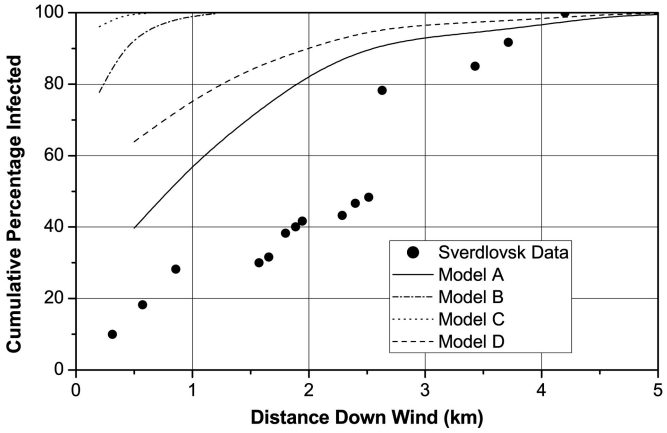

Fig. 3. Spatial distribution of victims at Sverdlovsk.

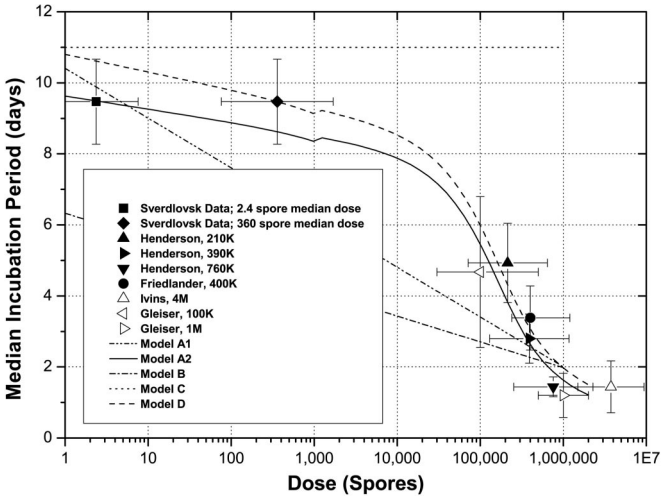

Fig. 4. Median incubation period versus dose. The kink in the middle of the curves for models A2 and D arises because the Sverdlovsk victims are assumed to have been exposed to an anthrax strain with an ID_{50} of ≈8,600 spores, whereas the nonhuman primates in the studies cited here were exposed to the Ames strain with an ID_{50} of ≈55,000 spores. Hence, the portion of the curve to the left of 1,000 spores assumes the lower ID_{50} value and the portion to the right assumes the higher ID_{50} value, thus causing a slight translation of the curve at 1,000 spores. Nonhuman primate data from Ivins *et al.* (33) and Gleiser *et al.* (27) (i.e., the open data points in Fig. 4) are shown for rough comparison only because either the number of nonhuman primates was too small or the time to death was not provided in these studies.

the Sverdlovsk incident necessarily produces a very small infected region because, by definition, only 81 people can be included inside the curve. For Chkalovsky, with a population density of ≈3,000 people per km^2, the area inside this curve would have to be quite small, on the order of 0.03 km^2 (19). The isopleths for models B and C, which have steeper dose–response curves, are compressed and extend only a short distance from the release point. Consequently, they are inconsistent with the extended spatial distribution of victims observed in the Sverdlovsk outbreak. Therefore, models A and D are the most accurate dose–response curves. Note that dose–response curves, which exhibit a threshold for infection, like step-function dose–response curves, are contraindicated by the Sverdlovsk data because they cannot produce extended spatial distributions of infected victims.

Model A predicts that 50% of the victims received less than approximately two spores (geometric mean $\mu = 2.4$ spores, geometric SD $d = 3.2$, i.e., 95% of the people were exposed to a dose between μ/d^2 and μd^2 spores). Model D predicts that 50% of the victims received $<\approx$360 spores (geometric mean $\mu = 360$, geometric SD $d = 4.7$). Thus, the victims at Sverdlovsk either received on the order of 1–10 spores (model A) or between 100–2,000 spores (model D), which is in good agreement with Meselson's estimates (7, 21). Fig. 11, which is published as supporting information on the PNAS web site, illustrates the predicted cumulative distribution of victims as a function of the number of spores to which individuals were exposed for each model. As this analysis shows, most of the victims at Sverdlovsk were exposed to doses far below the ID_{50} value.

Temporal Progression of Inhalation Anthrax

Current understanding of the incubation period for human inhalation anthrax is based largely on nonhuman primate experiments conducted over the past 50 years. Human data are relatively rare. Industrial exposure to contaminated wool and other animal products typically causes cutaneous anthrax, and the few inhalation cases on record resulted from chronic industrial exposure, thus precluding an accurate determination of the time of exposure and, hence, the incubation period (22).

Similarly, one cannot infer the dose to which victims were exposed for the 11 cases of inhalation anthrax resulting from contaminated letters in the United States in fall 2001 because, although the approximate date of exposure can be determined, and the strain type (Ames) and particle size (<5 microns) are known, the process by which spores were disseminated, opening a contaminated letter or having a contaminated letter pass through a mail sorting machine, does not allow one to determine human exposures accurately because too many imponderables affect the answer, e.g., the amount and size distribution of the material contained in each envelope, the manner in which it was opened, the indoor air velocity field, and human disturbances of this field (23). Hence, the dose to which the victims were exposed is largely indeterminate. The prodromal and fulminant phases of inhalation anthrax can be illuminated with these data, although in most cases prophylactic treatment occurred, which complicates ones ability to determine the natural course of the disease in the absence of medical treatment (24).

The Sverdlovsk accident, on the other hand, does allow one to determine the low-dose incubation period because the time of exposure has been estimated to within a fraction of a day (assuming that spore reaerosolization did not occur to an appreciable extent), the *B. anthracis* strains, possibly including up to four, released at Sverdlovsk were virulent strains used in the Soviet biological weapons program at the time (25), their particle size must have been $<\approx$5–10 microns for the cloud to have reached victims located several kilometers down wind, and the dose to which people were exposed can be estimated by simulating the release by using an atmospheric dispersion model, as discussed above. For the purpose of determining the incubation period, the release is assumed to be instantaneous, i.e., short compared to the victim's mobility.

According to the canonical wisdom, inhalation anthrax takes ≈1–5 days to incubate (2, 10). However, the Sverdlovsk data suggests that the median incubation period could be as long as 10–11 days (refs. 7–9). This discrepancy can be explained by assuming the incubation period for inhalation anthrax is dose-dependent. Incubation periods for many diseases vary inversely with the exposed dose (26). Gleiser (27) noted that the incubation period for inhalation anthrax appeared to be dose-dependent, and Anno has shown that Tularemia and Q-fever have incubation periods that appear to depend linearly on the logarithm of the exposed dose (28).

After the pioneering work of Sartwell (29), it is common to assume that incubation periods follow a log-normal distribution in time. This assumption fits the Sverdlovsk incubation data quite well. In this analysis, model A is assumed to have a log-normal incubation

Table 1. Incubation period distribution parameters

	Model A1		Model A2		Model B		Model C		Model D	
Measurement	Param.	Value (±SE)	Param.	Value (±SE)	Param.	Value (±SE)	Param.	Value (±SE)	Param.	Value (±SE)
Median incubation period										
	α	10.3 (±1.4)	θ	0.110 (±0.016)	α	6.33	α	11.0	θ	0.109 (±0.025)
	β	−1.35 (±0.25)	λ	8.84×10^{-6}	β	−0.725	β	0	λ	8.79×10^{-6}
			t_{lag}	1					t_{lag}	1
			t_2	2.06 (±0.24)					t_2	2.07 (±0.61)
			N_{thresh}	1×10^9					N_{thresh}	1×10^9
			σ	0.542 (±0.12)					σ	0.544 (±0.18)
Standard deviation										
	γ	0.804 (±0.56)	γ	0.804 (±0.56)	γ	0.17	γ	0.713		
	δ	−0.079 (±0.11)	δ	−0.079 (±0.11)	δ	0	δ	0		

period distribution, although one could pick other distributions. Models B and C also have log-normal incubation period distributions (12, 14). In log-normal models, the dose dependence of the incubation period is added exogenously by varying the median and SD of the distribution as a function of dose (Figs. 12 and 13, which are published as supporting information on the PNAS web site). The incubation distribution in model D is determined from the competing risks model (17). Fig. 4 illustrates the dose dependence of the median incubation period for all four models, along with estimates for the median incubation period in humans derived from maximum likelihood fits to the Sverdlovsk data and nonhuman primate data (27, 31–33). Unfortunately, early nonhuman primates studies of inhalation anthrax did not report the temporal evolution of the disease and, hence, do not shed light on the dose dependence of the incubation period (11, 19).

Two variations of model A are shown in Fig. 4. Model A1 assumes the median incubation period and the SD of the log-normal incubation period distribution vary linearly with the logarithm of the exposed dose, as discussed in Supporting Information. Model A2 assumes the median incubation period has the same form as the median incubation period in model D, with the exception that model A2 assumes the Model A dose–response curve and, hence, predicts that the mean (geometric) dose to which Sverdlovsk victims were exposed was ≈2.4 spores, whereas model D uses the model D dose–response curve with the resulting prediction that the Sverdlovsk victims were exposed to a mean (geometric) dose of ≈360 spores (unpublished data). The dose dependence of the SD in model A2 is the same as in model A1.

Model B assumes a log-linear dose dependence for the median incubation period, with a slope about half that for model A1, and a constant SD (12). Model C assumes the median incubation period and the SD are constant, independent of dose (14). The incubation period distribution for model D is a modified version of a model developed by Brookmeyer *et al.* (unpublished data). Model D is noteworthy because the dose dependence of the incubation period is derived *ab initio*.

The parameter values for these models are given in Table 1, along with estimates for the SEs (in parentheses). These parameters refer to the equations for the dose dependence of the incubation period in models A1, A2, and D found in *Supporting Text* (see Figs. 14 and 15, which are published as supporting information on the PNAS web site, for additional details). The parameters for model A1 were derived from a least-square fit to the Sverdlovsk and nonhuman primate data shown in Fig. 4. The parameter values for models A2 and D were determined from maximum likelihood fits to the Sverdlovsk incubation data alone. The parameters for Models B and C are found in the literature.

The median incubation period predicted by model D (or model A2) fits the Sverdlovsk and nonhuman primate data better (R^2 = 0.93) than the log-linear dose-dependent assumption in model A1 (R^2 = 0.82), lending some credence to the modified Brookmeyer model. Clearly, model B does not fit the Sverdlovsk median incubation period and model C does not fit the high-dose nonhuman primate data. Thus, models A and D provide the most accurate representation of the incubation period for human inhalation anthrax, with model A2 providing a somewhat better fit than model A1. The absence of data in the mid-exposure range, i.e., at the ID_{50} level, limits one's ability to distinguish between models A1 and A2. Models A2 and D yield a median incubation period for the Sverdlovsk victims of 9.5 (±0.6) days.

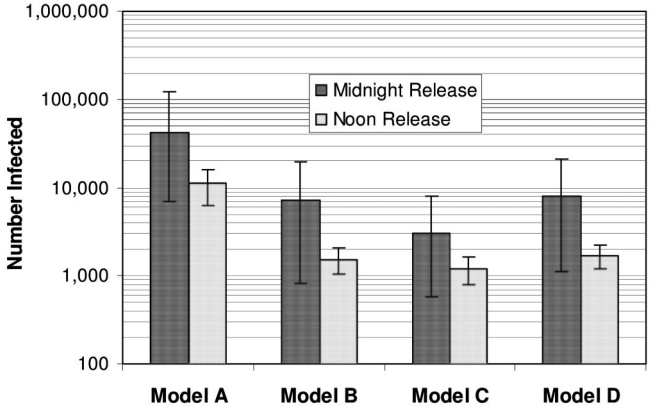

Fig. 5. Predicting casualties from an anthrax release.

Policy Implications

Returning to the four policy issues raised at the beginning, one now can assess the quantitative impact of assuming one anthrax model over another. Fig. 5 illustrates that model A predicts ≈10 times more casualties for an atmospheric anthrax release of fixed mass than the other models, as one might expect because of the low-dose tail of the dose–response curve.[¶] The height of each bar shows the average number of people that become infected and the error bars illustrate the 10 and 90 percentile values due to variability in the meteorological conditions from day to day (the variations are not normally distributed). Because models A and D give the best fit to the spatial distribution of victims at Sverdlovsk, these two models are useful bounding cases for the number of infected victims expected in a given attack scenario. Which one ultimately is more accurate will have to await further research on the low-dose infectivity of inhalation anthrax.

[¶]These calculations assume 1 kg of dry anthrax spores, with a density of 10^{11} spores/g and a 5% aerosolization efficiency for producing spores in the 1- to 5-μm size range, are released at midnight (or noon) during a typical July day in Washington, DC.

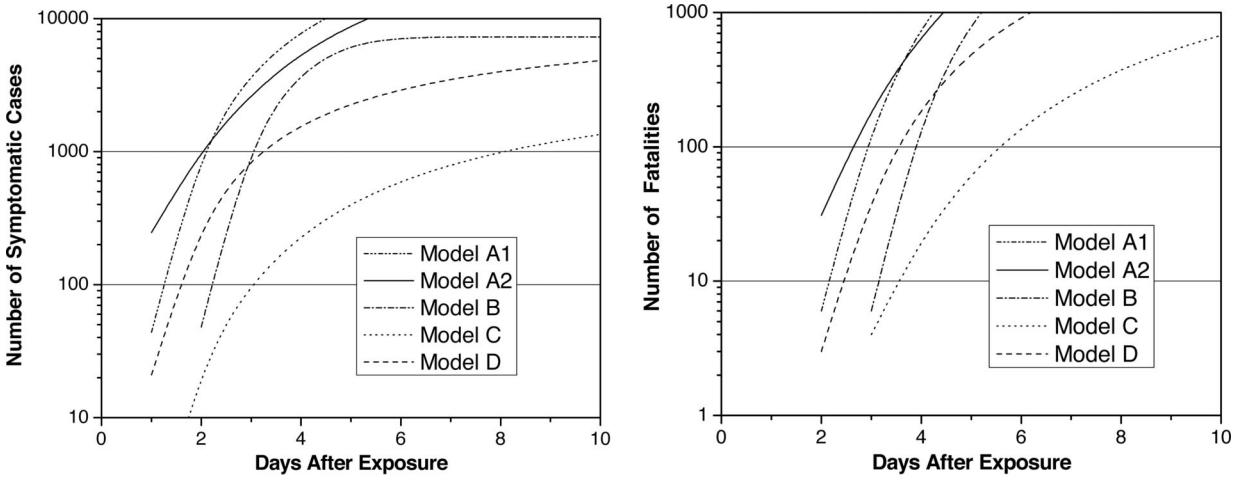

Fig. 6. Symptomatic (*Left*) and fatal cases (*Right*) versus time after exposure.

The severity of the decontamination problem also is influenced by the dose–response curve. For example, Wein *et al.* (30) analyzed the postattack anthrax decontamination problem by using the dose–response functions in models A and C, concluding that model A leads to a multibillion dollar cleanup problem, whereas the decontamination problem ceases to exist with model C because of the very small probability that reaerosolized anthrax spores would infect people in contaminated buildings, even when integrated over prolonged periods of time. Numerous uncertainties affect such calculations, not the least of which is the reaerosolization rate for micrometer-sized particles for relevant surface types. Nevertheless, the two most accurate dose–response functions for inhalation anthrax according to this analysis are models A and D, which have the highest likelihood of infection at low doses (see Fig. 1), suggesting that the indoor decontamination problem could be serious. Further research into dose–response functions and reaerosolization will be important to more accurately characterize cleanup strategies and costs.

The incubation period distribution and the distributions for the prodromal and fulminant stages of the disease allows one to predict when victims will become symptomatic and when they will begin to die after a given exposure, thus allowing one to predict when astute physicians might be able to recognize inhalation anthrax based on clinical presentation. If a blood culture is taken at this time, standard laboratory practice suggest that confirmation of inhalation anthrax might come within 24 h of the first few symptomatic cases, although this time will shorten as new diagnostic technologies become available. Fig. 6 shows the different model predictions for the number of symptomatic victims and the number of fatalities as a function of the time after exposure for the Washington, D.C., release mentioned above. Models A1, A2, and D predict 44, 247, and 21 symptomatic cases, respectively, 1 day after the release.

The time at which fatalities first appear is a more reliable warning indicator because most of the early symptoms of inhalation anthrax are similar to those for other infectious diseases, making a differential diagnosis difficult during flu season, for example. The first deaths occur on the second day, with models A1, A2 and D predicting ≈6, 31, and 3 fatalities, respectively, on the second day after the release.

Thus, if the release is large enough to infect ≈42,000 people, assuming model A, or 8,000 people, assuming Model D, an optimistic assessment suggests that clinical diagnosis of the first few symptomatic victims or fatalities could provide warning within ≈2 days of an anthrax release. Whether this conclusion is accurate depends critically on the early time tail of the incubation period distribution, particularly at high-dose exposures, the early time tail of the prodromal and fulminant period distributions, and the medical community's capability for differential diagnosis in the presence of a potentially large background of cases with flu-like symptoms. Considerable uncertainty exists in the early time tails of these disease-phase distributions. Consequently, one should interpret these results with care. More accurate experimental data will be required to improve these predictions.

Finally, the efficacy of medical intervention depends on its speed relative to the rate at which victims become symptomatic, because medical treatment is most effective if delivered before the onset of symptoms or shortly thereafter. Fig. 7 illustrates the fraction of potential victims that can, in principle, be saved as a function of the time at which medical intervention begins. Assuming that models A2 (or A1) and D provide the most accurate depiction of the incubation distribution, >90% of the exposed population can be saved if treatment begins within 2–3 days after the release. (The maximum medical efficacy asymptotes at 93% because of assumptions embedded in the model.) Clearly, the sooner one can provide prophylaxis to the exposed population, the better.

The medical intervention posited here consists of antibiotic distribution to 95% of the exposed population, estimated for the 1-kg release in Washington, DC, discussed above to be ≈300,000 people for model A anthrax and ≈30,000 people for model D anthrax, over a period of two days (possibly followed by vaccina-

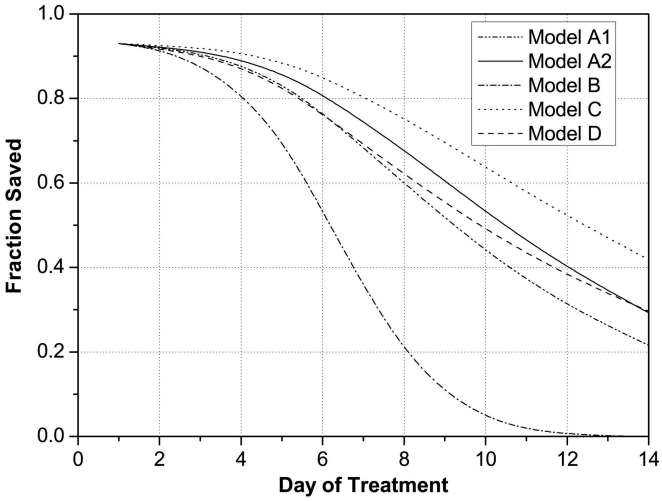

Fig. 7. Efficacy of medical intervention versus time after exposure.

tion), that antibiotic treatment before the onset of symptoms is 98% effective, and that postsymptomatic antibiotic treatment is relatively effective if delivered within ≈4 days of becoming symptomatic, assuming intensive medical care is available of the sort provided to the victims of the fall 2001 U.S. anthrax letter attacks (i.e., multidrug regimens and pleural fluid drainage) (24).

Fig. 7 should be interpreted with care because it is based on optimistic assumptions, given current U.S. preparedness, of the detection time, the speed with which medical logistics can deliver antibiotics to distribution sites, the speed with which people can be processed at distribution sites, especially if a large number of people who have not been exposed demand treatment, compliance over time with antibiotic regimens, and the effectiveness of antibiotic and vaccine treatments. Note that as the detection time is reduced, more time is available to implement medical prophylaxis. Real-time detection is not required, but detection within a fraction of a day is desirable. To achieve levels of protection $> 90\%$, policies must be implemented to reduce the fraction of people that do not receive prophylaxis (assumed here to be 5% of the exposed population) or that do not adhere to the full antibiotic regimen over time.

Discussion

Of the four models for human inhalation anthrax examined here, models A (A1 and A2) and D come closest to predicting the spatial and temporal distribution of human anthrax cases observed in the 1979 Sverdlovsk outbreak and the high-dose nonhuman primate incubation data available in the literature. Models A and D provide useful bounding predictions for the number of people infected in a given atmospheric release scenario, and all three models provide reasonable estimates for the temporal evolution of an outbreak, with the caveat that the early time predictions are suspect because of uncertainties in the early time tails of the incubation period distributions. This analysis is not sensitive to the exact ID_{50} value for micrometer-sized anthrax particles that, in any case, varies depending on strain type, culture preparation, and population susceptibility. However, regardless of ID_{50} value, the Sverdlovsk data clearly demonstrate that most of the victims were exposed to doses far below the ID_{50} value, which is likely to be the case for larger releases as well. Finally, given the uncertainty with which model parameters can be estimated from existing data, the general form of these results is to be trusted more than the precise numbers.

Log-normal models (i.e., models A1 and A2) provide an accurate empirical fit to incubation period distributions, as Sartwell (29) pointed out 50 years ago. However, model D is equally accurate and it has the virtue that it provides estimates for several underlying parameters on which the model is based, namely, the spore germination rate (8.8×10^{-6} per day), the spore clearance or destruction rate (0.109 per day), and the doubling time for *B. anthracis* replication in humans (2–4 h, depending on the bacterial threshold at which symptoms appear; see Fig. 15).

Clearly further research is needed to determine which of these two models provides the most accurate representation of human inhalation anthrax. Such research will allow policy makers to predict more accurately the likely consequences of a hypothetical atmospheric anthrax attack, the time at which such an attack might be detected by astute physicians, the efficacy of different medical intervention strategies, and the cost associated with postattack decontamination. Greater clarity with respect to these issues will help governments direct resources to those areas with the greatest payoff.

I thank Richard Danzig, Arthur Friedlander, Jeanne Guillemin, and Matthew Meselson for very helpful comments and discussions. Generous support for this research was provided by John D. and Catherine T. MacArthur Foundation Grants 99-57919-GSS and 02-69383-000-GSS and Carnegie Corporation Grant B4498.R11.

1. Guillemin, J. (2005) *Biological Weapons: From the Invention of State-Sponsored Programs to Contemporary Bioterrorism* (Columbia Univ. Press, New York).
2. Friedlander, A. M. (1997) in *Medical Aspects of Chemical and Biological Warfare, Textbook of Military Medicine, Part I*, ed. Zajtchuk, R. (Office of the Surgeon General, U.S. Army), pp. 467–478.
3. Watson A. & Keir, D. (1994) *Epidemiol. Infect.* **113,** 479–490.
4. Pile, J. C., Malone, J. D., Eitzen, E. M. & Friedlander, A. M. (1998) *Arch. Intern. Med.* **158,** 429–434.
5. Inglesby, T., Henderson, D. A., Bartlett, J. G., Ascher, M. S., Eitzen, E., Friedlander, A. M., Hauer, J., McDade, J., Osterholm, M. T., O'Toole, T., *et al.* (1999) *J. Am. Med. Assoc.* **281,** 1735–1745.
6. Inglesby, T. V., O'Toole, T., Henderson, D. A., Bartlett, J. G., Ascher, M. S., Eitzen, E., Friedlander, A. M., Gerberding, J., Hauer, J., Hughes, J., *et al.* (2002) *J. Am. Med. Assoc.* **288,** 2236–2252.
7. Meselson, M., Guilleman, J., Hugh-Jones, M., Langmuir, A., Popova, I., Shelokov, A. & Yampolskaya, O. (1994) *Science* **266,** 1202–1208.
8. Guillemin, J. (1999) *Anthrax: Investigation of a Deadly Outbreak* (Univ. of California Press, Berkeley).
9. Brookmeyer, R., Blades, N., Hugh-Jones, M. & Henderson, D. A. (2001) *Biostatistics* **2,** 233–247.
10. Franz, D. R., Jahrling, P. B., Friedlander, A. M., McClain, D. J., Hoover, D. L., Bryne, W. R., Pavlin, J. A., Christopher, G. W. & Eitzen, E. M. (1997) *J. Am. Med. Assoc.* **278,** 399–411.
11. Glassman, H. (1966) *Bacteriolog. Rev.* **30,** 657–659.
12. Anno, G. H. & Bloom, R. (1998) *Anthrax Effects Model* (Pacific Sierra Research Corp., Santa Monica, CA) PSR Rep. 2773B.
13. Anno, G. H. (2001) *Susceptibility of Mammalian Species to Inhalation of Aerosolized Bacillus Anthracis Spores* (Veridian Systems Division, Santa Monica, CA).
14. Wein, L. M., Craft, D. L. & Kaplan, E. H. (2003) *Proc. Natl. Acad. Sci. USA* **100,** 4346–4351.
15. Druett, H. A. (1952) *Nature* **170,** 288.
16. Haas, C. N. (2002) *Risk Analysis* **22,** 189–193.
17. Brookmeyer, R., Johnson, E. & Barry, S. (2005) *Stat. Med.* **54,** 531–542.
18. Webb, G. F. & Blaser, M. J. (2002) *Proc. Natl. Acad. Sci. USA* **99,** 7027–7032.
19. Druett, H. A., Henderson, D. W., Packman, L. & Peacock, S. (1953) *J. Hyg.* **51,** 359–371.
20. Alibek, K. (1999) *Biohazard* (Random House, New York).
21. Meselson, M. (2001) *Applied Science and Analysis Newsletter* **48,** 20–21.
22. Brachman, P. S., Kaufmann, A. F. & Dalldorf, F. G. (1966) *Bacteriolog. Rev.* **30,** 646–657.
23. Agranovski, I. E., Pyankov, O. V. & Altman, I. S. (2005) *Aerosol Sci. Technol.* **39,** 1048–1055.
24. Holty, J. C., Bravata, D. M., Liu, H., Olshen, R. A., McDonald, K. M. & Owens, D. K. (2006) *Ann. Intern. Med.* **144,** 270–280.
25. Jackson, P. J., Hugh-Jones, M. E., Adair, D. M., Green., G., Hill, K. K., Kuske, C. R., Grinberg, L. M., Abramova, F. A. & Keim, P. (1998) *Proc. Natl. Acad. Sci. USA* **95,** 1224–1229.
26. Tigertt, W. D., Benenson, A. S. & Gochenour, W. S. (1961) *Bacteriolog. Rev.* **25,** 285–293.
27. Gleiser, C. A., Berdjis, C. C., Hartman, H. A. & Gochenour, W. S. (1963) *Br. J. Exper. Pathol.* **44,** 416–426.
28. Anno, G. H. & Deverill, A. P. (1998) *Consequence Analytic Tools for NBC Operations* (Def. Special Weapons Agency, Alexandria, VA) Report DSWA-TR-97-61-V1.
29. Sartwell, P. (1950) *Am. J. Hyg.* **51,** 310–318.
30. Wein, L. M., Liu, Y. & Leighton, T. J. (2005) *Emerging Infect. Diseases* **11,** 69–76.
31. Henderson, D. W., Peacock, S. & Belton, F. C. (1956) *J. Hyg.* **54,** 28–36.
32. Friedlander A. M., Welkos, S. L., Pitt, M. L., Ezzell, J. W., Worsham, P. L., Rose, K. J., Ivins, B. E., Lowe, J. R., Howe, G. B., Mikesell, P., *et al.*(1993) *J. Infect. Dis.* **167,** 1239–1243.
33. Ivins, B. E, Fellows, P. E., Pitt, M. L. M., Estep, J. E., Welkos, S. L., Worsham, P. L. & Friedlander, A. M. (1996) *Salisbury Medical Bulletin-Special Supplement* **87,** 125–126.